

U

O

W

# A Geant4 Simulation Study for *in-vivo* Range Verification in Proton Therapy

Melek Zarifi<sup>1</sup>, Yujin Qi<sup>1</sup>, Susanna Guatelli<sup>1</sup>, David Bolst<sup>1</sup>, Dale Prokopovich<sup>2</sup>, Anatoly Rosenfeld<sup>1</sup>

<sup>1</sup> Centre for Medical Radiation Physics, University of Wollongong, Wollongong NSW Australia

<sup>2</sup> Australian Nuclear Science and Technology Organisation, Lucas Heights NSW Australia

CENTRE FOR  
MEDICAL  
RADIATION  
PHYSICS



UNIVERSITY  
OF WOLLONGONG  
AUSTRALIA

# Hadron Therapy

- The advantage of hadron therapy (protons, carbon, helium ions) compared to conventional X-ray radiotherapy is the localised energy deposition in the **Bragg Peak (BP)**.
- But due to the sharp BP distal fall-off, tumour targeting must be precise, to avoid irradiation of normal tissue.
- High precision hadron therapy requires *in-vivo* **beam range verification** techniques to verify dose delivery while assuring safety margins during the treatment process.

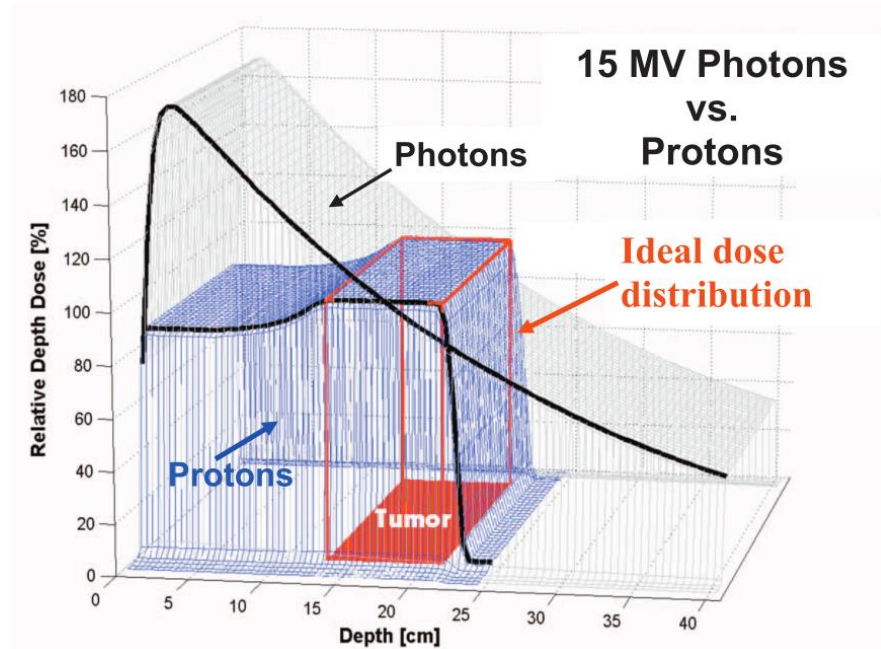
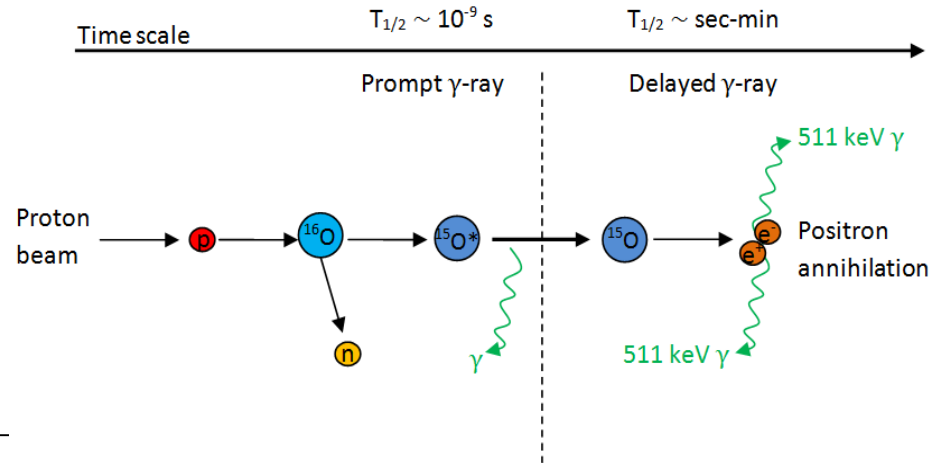


Figure showing comparison between photon and proton beams.  
Smith AR 2009.

# Beam Range Verification: Prompt Gamma

- There are various beam monitoring techniques, PET is used to detect delayed gammas from  $\beta^+$  emitting radioisotopes ( $^{11}\text{C}$ ,  $^{13}\text{N}$ ,  $^{15}\text{O}$ ).
  - Does not offer real-time monitoring, biological washout for soft tissue, organ motion, difficulties in image co-registration
- Prompt gamma (PG) imaging is a novel technique which can provide a real-time signal for beam range verification, but this technology is still unavailable for clinical applications.
- PG is emitted in the decay process from an excited nucleus following proton-nuclear interaction.
- PG technique unique advantages:
  - Enable on-line treatment monitoring in real time
  - Provide high accuracy of range verification ( $\sim 1\text{mm}$ ), with close correlation between proton range and PG production position
  - Discrete spectral lines in PG emission contain information of tissue composition



# Literature Review

## Characteristics and feasibility of prompt gamma

- **Studied PG characteristics and feasibility** as range verification technique (Min *et al* 2006, Polf *et al* 2009a, Peterson *et al* 2010, Frandes *et al* 2010). Use emitted spectrum to determine **elemental composition** of irradiated tissue (Polf *et al* 2009b, Polf *et al* 2013).

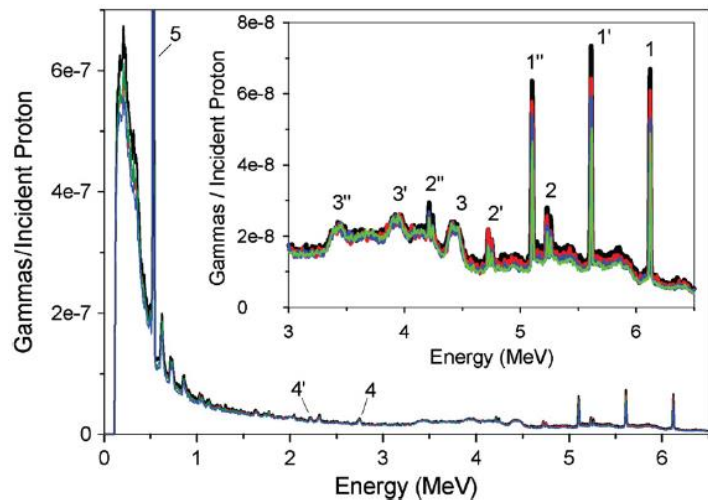


Figure 4. Measured prompt gamma spectra per incident proton emitted from the irradiated water (black line), and the 25 g (red line), 75 g (blue line), and 130 g (green line) sucrose solutions. The spectra show the prompt gamma, single escape, and double escape emission peaks for  $^{16}\text{O}$  (1, 1', 1'', 4, 4'),  $^{15}\text{O}$  (2, 2', 2''), and  $^{12}\text{C}$  (3, 3', 3''), as well as the positron annihilation gamma peak (5).

< Polf *et al*, *Measurement of characteristic prompt gamma rays emitted from oxygen and carbon in tissue-equivalent samples during proton beam irradiation*, 2013.

Verburg *et al*, *Energy- and time-resolved detection of prompt gamma-rays for proton range verification*, 2013. >

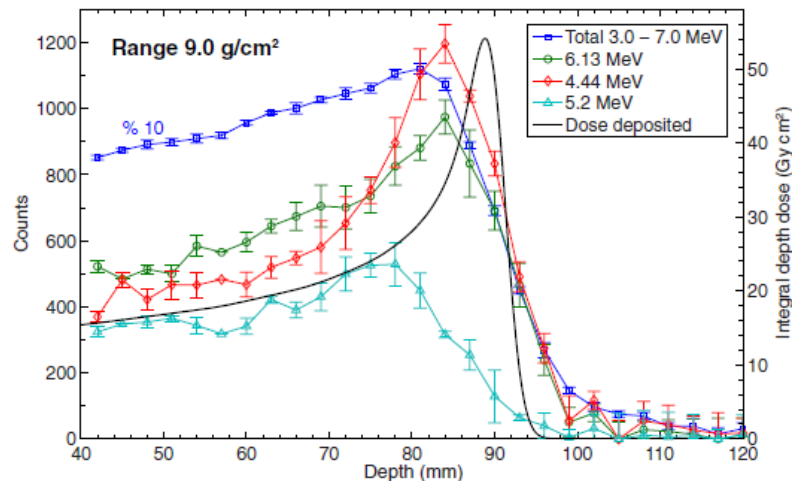


Figure 7. Energy-integrated ( $\square$ ) and discrete ( $\circ$ ,  $\diamond$ ,  $\Delta$ ) prompt gamma-ray emissions along the path of proton pencil-beams in water. For proton ranges of 9.0, 16.0 and 23.0  $\text{g cm}^{-2}$ , shown is the mean and  $\pm 1\sigma$  statistical uncertainty of five measurements with  $10^{10}$  incident protons per measurement point. The lines connecting the points serve to guide the eye. The dose deposited by  $10^{10}$  protons is shown for reference, which is based on the clinically commissioned depth-dose curve.

# Literature Review

## Detector designs for PG imaging

• **Passive (mechanical) collimation:** collimated PG camera (Min *et al* 2006, Testa *et al* 2010), pinhole, knife-edge shaped slit placed perpendicular to beam direction (Bom *et al* 2012, Smeets *et al* 2012).

• **Active (electronic) collimation:** Compton cameras (Kormoll *et al* 2011), double-scattering cameras (Peterson *et al* 2010, Richard *et al* 2011) use Compton kinematics to trace gamma source.

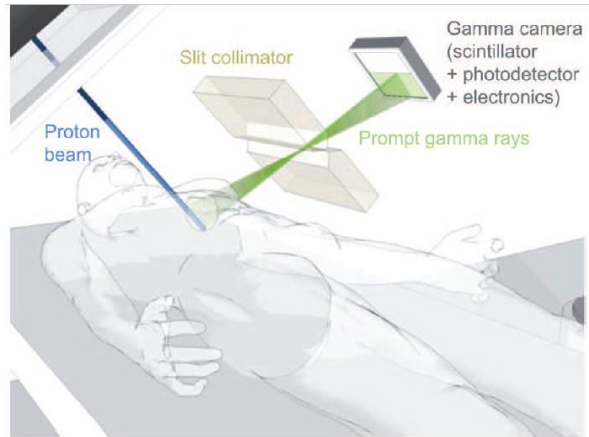


**Figure 1.** The slit camera concept: a slit collimation gives a 1D projection of prompt gamma emissions along the beam path on a scintillation detector.

cf. **Figure 4** for the two-plane camera. The Compton equation (41) relates the scattering angle  $\theta$  to the initial ( $E_\gamma$ ) and final ( $E_\gamma'$ ) photon energies:

$$\begin{aligned} E_\gamma &= L_s + L_a \\ E_\gamma' &= L_a \\ \cos\theta &= 1 - m_e c^2 \left( 1/E_\gamma' - 1/E_\gamma \right) \end{aligned} \quad (1)$$

where  $L_s$  and  $L_a$  are the energies released in scatterer and absorber, respectively, and  $m_e c^2 = 511$ -keV is the electron rest energy. In contrast to a slit camera, no collimation is needed

Gonzalez et al, *Compton camera and prompt gamma ray timing: two methods for in vivo range assessment in proton therapy*, 2016.

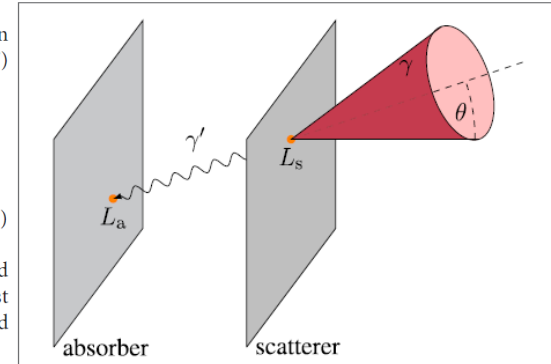
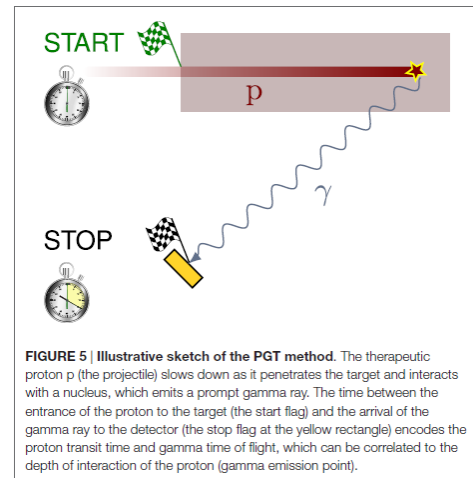


**FIGURE 4 | Incoherent scattering event in a two-plane Compton camera.** The cone surface contains the possible incidence directions (any generatrix) of the initial photon ( $\gamma$ ). It interacts with the scatterer plane and deposits an energy  $L_s$ . The scattered photon ( $\gamma'$ ) releases the rest of the energy  $L_a$  in the absorber. The line connecting both interaction points (in orange) is the propagation direction of  $\gamma'$ . This defines the axis (directrix) of the aforementioned cone, with half-opening (scattering) angle  $\theta$  and vertex at the scatterer point.

# Literature Review

## Other beam monitoring techniques

- **Prompt gamma spectroscopy (PGS):** Discrete excited states of nuclei to monitor beam range and assess elemental composition of irradiated tissue (Verburg *et al* 2014).
- **Prompt gamma timing (PGT):** TOF distributions encode information about spatial emission point (Golnik *et al* 2014). TOF also for reducing neutron background (Testa *et al* 2008, Biegun *et al* 2012).
- **Prompt gamma peak integration (PGPI):** Integral and mean of TOF peak used to detect deviations from the prescribed treatment (Krimmer *et al* 2017).



Gonzalez *et al*, 2016.

Golnik *et al*, *Range assessment in particle therapy based on prompt gamma-ray timing measurements*, 2014.

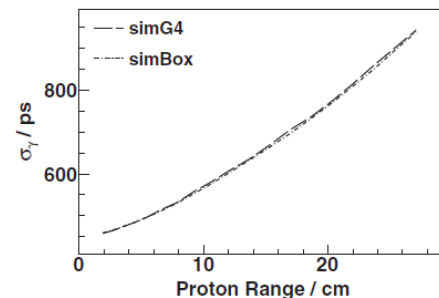
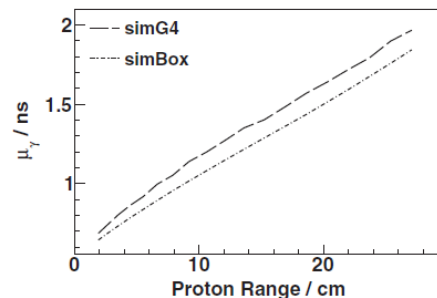
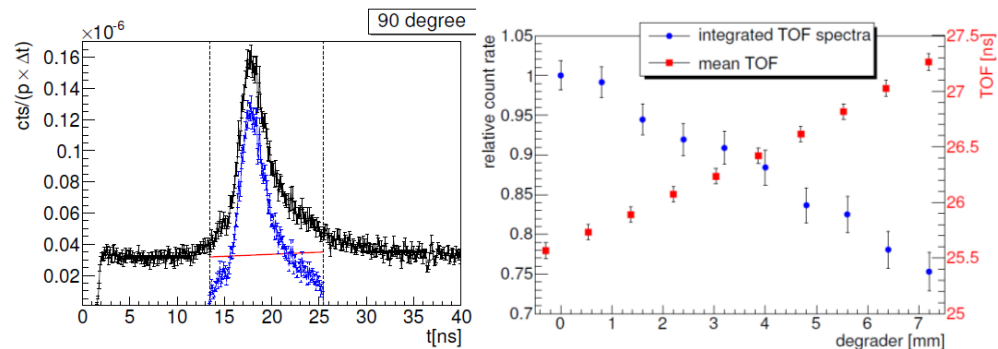


**Figure 12.** Range-dependent mean value  $\mu_\gamma$  (left) and standard deviation  $\sigma_\gamma$  (right) of modeled prompt  $\gamma$ -ray PGT spectra. The target material is PMMA. The proton energies are in the range of 50 MeV up to 230 MeV, corresponding to proton ranges from 2 cm up to 27 cm. The assumed system time resolution  $\sigma_\Sigma$  is 450 ps.

Krimmer *et al*, *A cost-effective monitoring technique in particle therapy via uncollimated prompt gamma peak integration*, 2017.

# Research Goal

- Main challenges of PG imaging are the absence of optimised PG detection methodology and technology.
  - Capable of measuring **high-energy** gamma rays, high count rates, with suitable efficiency and precision.
  - Technique to reduce background for **improving signal-to-noise** ratio.
  - Technology for **fast timing** of gamma detection and electronics.
- **Goal:** investigate and develop a novel *in-vivo* dose verification technique using PG signals to enable on-line treatment monitoring in particle therapy.
  1. Monte Carlo simulations to (1) investigate PG **emission and detection characteristics** and (2) determine optimal system for **uncollimated PG detection** using TOF information for BP tracking.
  2. Develop detector/s, optimise system. Main requirement is good **energy and timing resolution**.
  3. Test/verification.

# Conclusion

- The **energy spectra** of gamma emission is characteristic to the elemental composition of the phantom material. Prominent PG emission lines are 4.44, 5.21, 6.13 MeV from  $^{12}\text{C}$ ,  $^{15}\text{O}$  and  $^{16}\text{O}$ , respectively.
- **PG rays** offer improved correlation to the BP distal fall-off compared to total gamma emission.
- The **preferential position** for PG detection is slightly backward peaked, for proton beam, and normally, for  $^{12}\text{C}$  beam, relative to the BP position.
- **PG TOF spectra** changes with beam energy, the peak mean and integral increase with higher beam energy – the potential for a simple, uncollimated means of BP tracking.
- **Next stage of simulations:**
  - Different phantom shapes (e.g. cylinder) and materials (e.g. plastic, tissue-equivalent).
  - Model PG energy and TOF response of realistic scintillation detectors positioned around the phantom.

U

O

W

Thank you

CENTRE FOR  
MEDICAL  
RADIATION  
PHYSICS



UNIVERSITY  
OF WOLLONGONG  
AUSTRALIA

# Acknowledgements

- We would like to thank the University of Wollongong Information Management & Technology Services (IMTS) for computing time on the UOW High Performance Computing Cluster.
- This research has been conducted with the support of the Australian Government Research Training Program Scholarship.

# References

- Smith AR, *Vision 20/20: Proton therapy*, Med. Phys. 2009, 36: pp 556-568
- Min CH et al, *Prompt gamma measurements for locating the dose fall-off region in proton therapy*, Appl. Phys. Lett. 2006, 89: pp 1835-17
- Polf JC et al, *Prompt gamma-ray emission from biological tissues during proton irradiation: a preliminary study*, Phys. Med. Biol. 2009a, 54: pp 731-743
- Peterson SW et al, *Optimizing a three-stage Compton camera for measuring prompt gamma rays emitted during proton radiotherapy*, Phys. Med. Biol. 2010, 55: pp 6841-6856
- Frandes M et al, *A tracking Compton-scattering imaging system for hadron therapy monitoring*, IEEE Trans. Nucl. Sci. 2010, 57: pp 144-150
- Polf JC et al, *Measurement and calculation of characteristic prompt gamma ray spectra emitted during proton irradiation*, Phys. Med. Biol. 2009b, 54: pp 519-527
- Polf JC et al, *Measurement of characteristic prompt gamma rays emitted from oxygen and carbon in tissue-equivalent samples during proton beam irradiation*, Phys. Med. Biol. 2013, 58: pp 5821-5831
- Verburg JM et al, *Energy- and time-resolved detection of prompt gamma-rays for proton range verification*, Phys. Med. Biol. 2013, 58: pp L37-L49
- Verburg JM et al, *Proton range verification through prompt gamma-ray spectroscopy*, Phys. Med. Biol. 2014, 59: pp 7089-7106
- Testa M et al, *Monitoring the Bragg peak location of 73 MeV/u carbon ions by means of prompt g-ray measurements*, Appl. Phys. Lett. 2008, 93: 093506
- Bom V et al, *Real-time prompt gamma monitoring in spot-scanning proton therapy using imaging through a knife-edge shaped slit*, Phys. Med. Biol. 2012, 57: pp 297-308
- Smeets J et al, *Prompt gamma imaging with a slit camera for real-time range control in proton therapy*, Phys. Med. Biol. 2012, 57: pp 3371-3405
- Kormoll T et al, *A Compton imager for in-vivo dosimetry of proton beams – A design study*, Nucl. Instrum. Methods Phys. Res. 2011, 626-627: pp 114-119
- Richard MH et al, *Design guidelines for a double scattering Compton camera for prompt- $\gamma$  imaging during ion beam therapy: a Monte Carlo simulation study*, IEEE Trans. Nucl. Sci. 2011, 58: pp 87-94
- Perali I et al, *Prompt gamma imaging of proton pencil beams at clinical dose rate*, Phys. Med. Biol. 2014, 59: pp 5849-5871
- Gonzalez FH et al, *Compton camera and prompt gamma ray timing: two methods for in vivo range assessment in proton therapy*, Front. in Onc. 2016, 6: pp 1-13
- Biegun AK et al, *Time-of-flight neutron rejection to improve prompt gamma imaging for proton range verification: a simulation study*, Phys. Med. Biol. 2012, 57: pp 6429-6444
- Golnik C et al, *Range assessment in particle therapy based on prompt gamma-ray timing measurements*, Phys. Med. Biol. 2014, 59: pp 5399-5422
- Krimmer J et al, *A cost-effective monitoring technique in particle therapy via uncollimated prompt gamma peak integration*, 2017, DOI: 10.1063/1.4980103